Journal of Applied Geophysics (Cairo) Vol. 21, Issu.2, September (2022) (p.p., 1-10)

ISSN: 1687-1251

Egyptian Society of Applied Petrophysics

Journal of Applied Geophysics (Cairo)

Journal home page: https://jag.journals.ekb.eg/

Original Article

Petrophysical analysis for the well logging data; A case study from West Wadi El Rayan, Abu El-Gharadig basin, Western Desert, Egypt

Mohannad O. AboBakr[*1], Walid M. Mabrouk[1] and Ahmed M. H. Metwally[1]

[1] *Geophysics Department, Faculty of Science, Cairo University, Giza, Egypt*

ARTICLE INFO

Keywords:
Petrophysical analysis
Abu El-Gharadig basin
hydrocarbon prospect
Egypt

Received 9 June 2022
Revised 1 August 2022
Accepted 15 August 2022
Published 1 September 2022

ABSTRACT

The purpose of this paper is mainly to apply a complete workflow for a petrophysical evaluation to enhance and quantify hydrocarbon prospect and productivity of West Wadi El Rayan field in Abo El Gharadig Basin, Western Desert, Egypt through the quantitative interpretation of the logging data for WD38-1 well. The litho-saturation model will be created for WD38-1 well, so that at each depth, the volume of shale, matrix, water and hydrocarbon could be determined. This model provides a direct technique for the quantitative interpretation for the petrophysical parameters, such as shale volume (Vsh), porosity ($\emptyset$) and fluid saturations (Sw and Sh), which are the most important for the geologists, geophysicists, petrophysicists and petroleum engineers.

1. Introduction

This study introduces a review for the main petrophysical parameters, calculated from the conventional well logging data. A workflow (Fig.1) is represented to design the litho-saturation model, which is the desired output from this study. To construct the litho-saturation model, the volume of each of its internal components (rocks and fluids) should be calculated. First, the shale volume (V_{sh}) calculations is followed by the porosity ($\emptyset$) calculations, after that by adding the shale volume to the porosity and subtracting them from the total volume and the volume of matrix (V_{ma}) will be estimated. Then, the water and hydrocarbon saturations (S_w & S_h), which need the determination of the water resistivity (R_w) to be calculated. Finally, the bulk volumes of the fluids either water or hydrocarbon will be calculated.

[*] Corresponding author at: *Geophysics Department, Faculty of Science, Cairo University, Giza, Egypt*

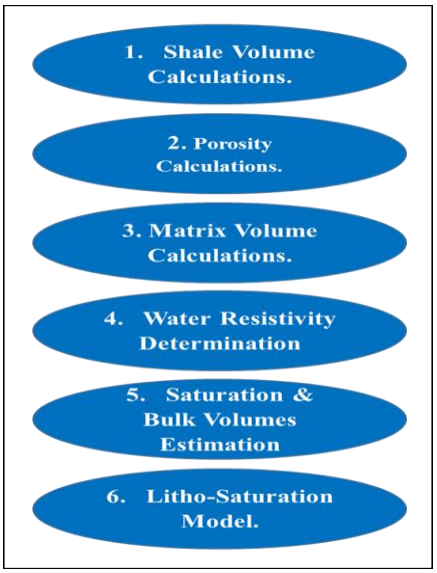

Fig.1. A workflow to construct the litho-saturation model.

2. General Geologic setting

The Western Desert of Egypt is a district that lies west of the River Nile, the width of the Western Desert extends from 800 km at the north to 1000 km at the south away from the Nile Valley at the east to the Libyan border at the west. Its length is about 1200 km from the Mediterranean shoreline at the north to the Sudan border at the south. It is named - in contrast to the Eastern Desert - which extends east from the River Nile to the Red Sea.The Western Desert is mostly rocky desert, though an area of sandy desert, known as the Great Sand Sea, lies to the west against the Libyan border. The desert covers an area of 680,650 km2 which is two-thirds of the land area of the country.

The study area is located at West Wadi El-Rayan filed (WWER) which located in the Western Desert at about 140 km South West of Cairo and 65 km South West of El-Fayoum. The study area lies between latitudes 29° 30`- 29° 50`N and longitudes 29° 50`- 30° 10`E, West Wadi El-Rayan area lies between Gindi Basin and at the east side and Abu El-Gharadig basin at the west side (Fig.3). According to Darwish (1992), several anticline structures, that can be related to the Syrian Arc inverted basins, are present across the stretch from the Gulf of Suez to the Western Desert passing along the Kattaniya high, Sharib-Sheiba platform, Qarun, Abu El-Gharadig, Alamein, Shushan and Matruh

3. Available data

The data consists of WD38-1 well which located at West Wadi El-Rayan (WWER) filed (Fig.3), which contain: Gamma-ray (GR) log, Neutron (($\emptyset_N$)) log, Density (ρ_b) log, resistivity (Res Deep, MSFL, Res Shallow) logs and photoelectric (PE) log, as well as detailed formation tops. The well drilled in the study area and the well results are shown in the Table (3a) The available 2D Seismic reflection data (Fig 3) contain five different surveys conducted over West Wadi El Rayain (WWER) area are summarized in the following tables (Table 3.a & b)

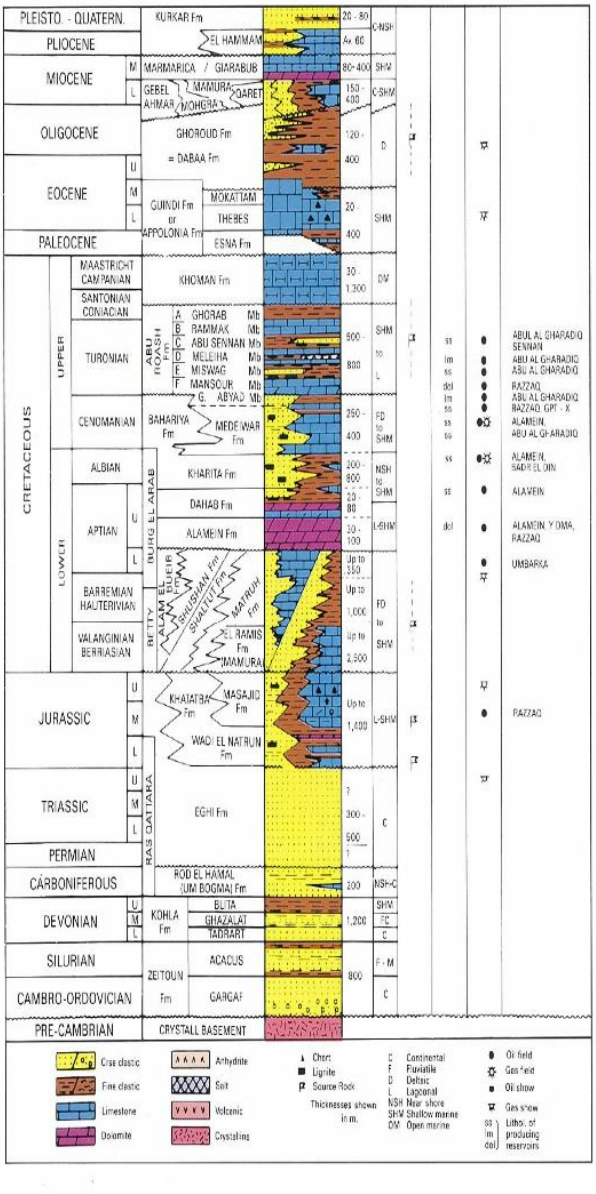

Fig.2. A generalized Litho-Stratigraphic column of the northern part of the Western desert (Said,1990; EGPC ,1992)

Table.3a. Well result for WD38-1 well

Well name	Company	Year	TD	MD	KBE	Formation reached	Shows/Formation reached	Status
WD 38-1	Gupco.	1974	2961	-2671	290	Jurassic	Good Oil shows in Bahariya Formation	Oil Shows

Table 3b. Summarized Acquisition parameters of the study area.

Survey	Year of Acquisition	Acquisition Company	Owner Company	Area	Source Type	Fold no.	Data Quality
SQ	1984	GSI	Shell	Qarun	Vibroseis	48	Fair
SQ	1985	CGG	Shell	Qarun	Vibroseis	72	Fair
WQ 85	1985	Western	Gapco	West Qarun	Vibroseis	48	Good
WQ86	1986	Western	Gapco	West Qarun	Vibroseis	48	Good
9603 HF-HG-HH-HI	1996	CGG	Repsol	East Bahariya	Vibroseis	60	Fair
9710 REB	1997	Geco Prakla	Repsol	East Bahariya	Vibroseis	80	Good

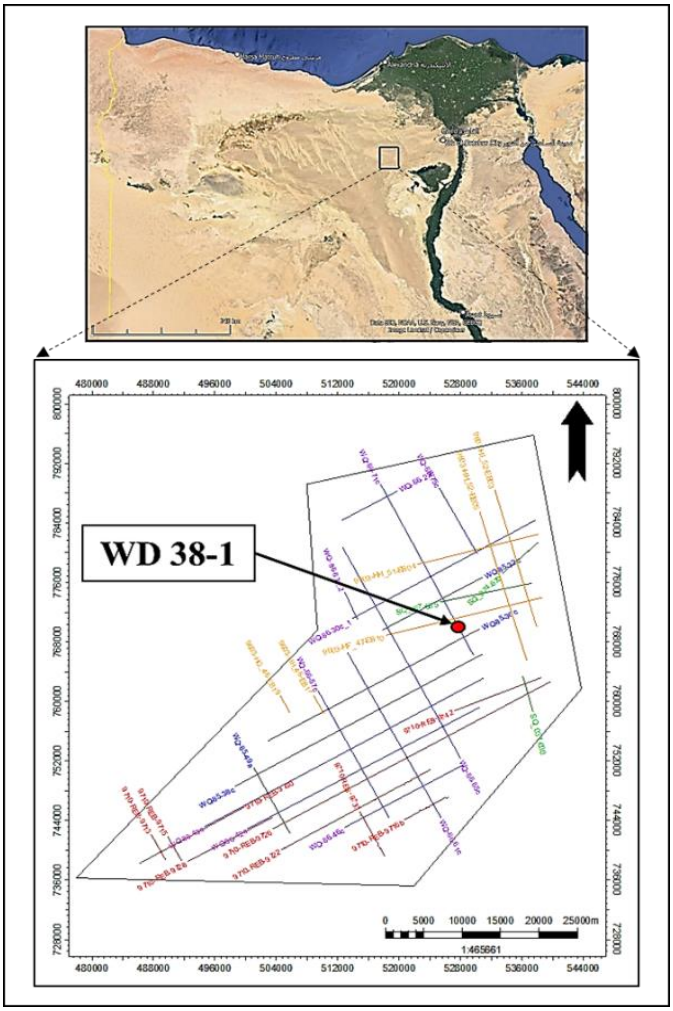

Fig.3. The study area and WD38-1 well location, West Wadi El Rayan Area, Western Desert, Egypt.

4. Petrophysical analysis

The workflow - discussed in Figure 1 - is applied on the well logs derived from WD38-1 well, located at Abu El-Gharadig basin, for formation evaluation and litho-saturation model.

4.1. Shale volume (V_{sh}) calculations

It is the first and most critical parameter to calculate. This is because all the other petrophysical parameters (effective porosity and water saturation) will be dependent on the volume of shale (V_{sh}).The volume of shale has a great impact in log interpretation. In a porous-permeable rock unit, if the volume of shale is under-estimated, the calculation of the effective porosity will be optimistic, while if the volume of shale is over-estimated, the calculation of the effective porosity will be pessimistic (Kamel and Mabrouk, 2003).

One of the most used equations for shale volume calculation, and the one we applied in our case study, is the linear gamma-ray index equation (4.1a).

$$I_{GR} = \frac{GR_{log} - GR_{min}}{GR_{max} - GR_{min}} \qquad (4.1a)$$

where; GR denotes the gamma-ray reading of the given depth-point, GRmin and GRmax are the gamma-ray values of the clean formation (minimum reading on the GR-log) and shale (maximum reading on the GR log), respectively (Asquith and Krygowski, 2004), (Asquith et al., 1982).
The shale volume (V_{sh}) was calculated from the GR log, using equation (4.1a) and Steiber correction (1970) was applied as shown in equation (4.1b). The GR-log and the corresponding shale volume for WD38-1 well are displayed in (Fig 4.1), as an example.

$$V_{sh} = \frac{0.5 * I_{GR}}{1.5 - I_{GR}} , \qquad \text{(Steiber, 1970)} \quad (4.1b)$$

where: V_{sh} is the volume of shale; GR_{log} is the gamma-ray reading; GR_{max} is the maximum gamma-ray (shale); GR_{min} is the minimum gamma-ray (clean sand or carbonate).

4.2. Porosity ($\emptyset$) calculations

The total porosity is calculated from the neutron ($\emptyset_N$) and density (ρ_b) logs, then the effective porosity ($\emptyset_{eff.}$) is calculated (**Hassan et al., 2019**), considering the shale volume (V_{sh}) and the shale porosity ($\emptyset_{sh}$). Fig (4.2) shows an example for calculating the total and effective porosities in WD38-1 well.

$$\emptyset_{Total} = \emptyset_{ND} = \frac{\emptyset_N + \emptyset_D}{2} \qquad (4.2a)$$

$$\emptyset_{eff} = \emptyset_{total} - (V_{sh} * \emptyset_{sh}) \qquad (4.2b)$$

Where: $\emptyset_{Total}$ *or* $\emptyset_{ND}$ is the total porosity or neutron porosity; $\emptyset_{eff}$ is the effective porosity; $\emptyset_{sh}$ is the porosity of shale; V_{sh} is the corrected shale volume.

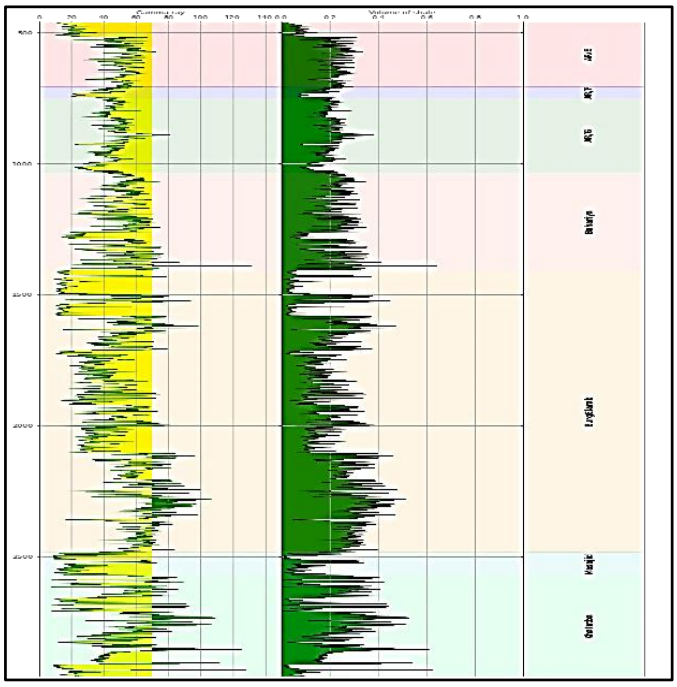

Fig.4.1. GR log and the calculated shale volume (Vsh) for WD38-1 well

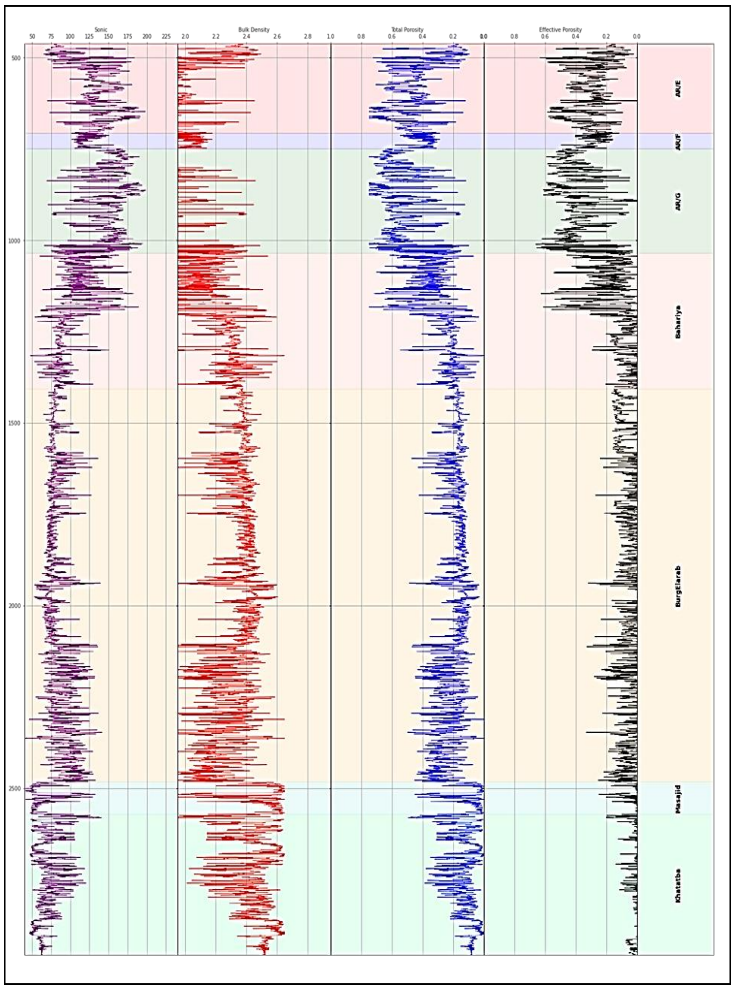

Fig.4.2. $\emptyset_N$ and ρ_b logs, and the calculated total and effective porosities for WD38-1 well.

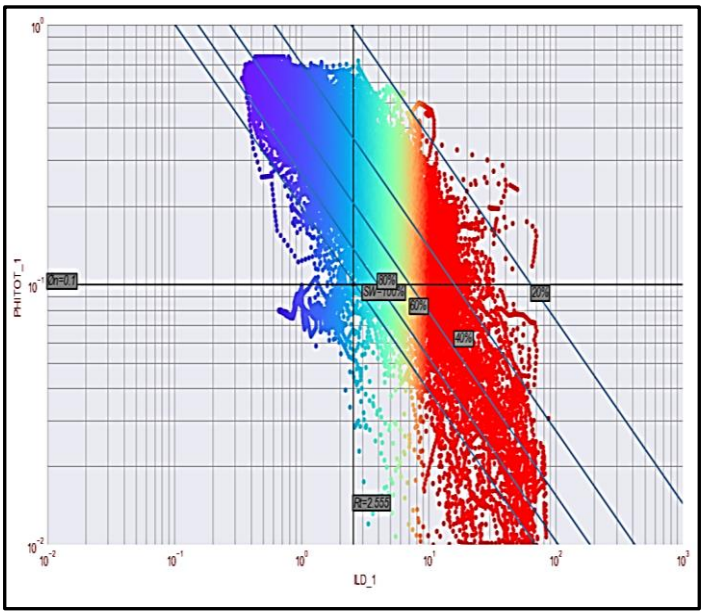

Fig.4.4. Picket's plot for WD38-1 well

Another method (Chikiban B. et al., 2022) is worked out to calculate the effective porosity by using the density tool, as:

$$\emptyset_{eff} = \emptyset_D - (V_{sh} * A) \qquad (4.2c)$$

Then calculating the density – derived porosity for the total and shale rocks, as;

$$\emptyset_D = \frac{\rho_m - \rho_b}{\rho_m - \rho_{fl}} \qquad (4.2d)$$

$$\emptyset_D = \frac{\rho_m - \rho_{sh}}{\rho_m - \rho_{fl}} \qquad (4.2e)$$

where:

ρ_m is the density of matrix, standard value (ρ_{ma} = 2.68 g /CM^{-3}); ρ_b s the density log value

ρ_{fl} is the density of pore fluids, standard value (ρ_f = 1.0 g /CM^{-3}); ρ_{sh} is the density of shale, from laboratories measurement; (ρ_{sh} = 2.42 g / CM^{-3}) V_{sh} is the volume of shale, in decimal; A is the shale correction.

4.3. *Matrix volume (V_{ma}) calculations*

By definition, the matrix volume (V_{ma}) could be estimated by subtracting the sum of the shale volume (V_{sh}) and the effective porosity ($\emptyset_{eff}$) from unity, The volume of rock can be reached from the summation of individual shale volume and matrix volume that calculated from individual tools, to get information for the total porosity by sabtracting rock volume from unity, as shown in equation (4.3).

$$V_{ma} = 1 - (V_{sh} + \emptyset) \qquad (4.3)$$

4.4. *Water resistivity (R_w) determination*

In this case study, Picket's plot, 1973. (Fig 4.4) is used to determine the water resistivity (R_w), where the porosity ($\emptyset_N$) values are plotted versus the deep resistivity (R_t) values on a log-log scale. Then by the line, which best fits the minimum values for both, represents the 100% water saturation. By choosing a value for the porosity ($\emptyset_N$) on the Y-axis and intersecting the line of the 100% water saturation, the corresponding value on the X-axis (R_t) will be the R_o. Then, the water resistivity could be calculated using equation (4.4).

$$R_o = F * R_w \qquad (4.4)$$

where:

R_o is the formation water resistivity at S_w=100%; F is the formation resistivity factor (F=$\emptyset^{-m}$); m is the cementation factor, the slope of the line, representing S_w=100% , equals (-1/m).

4.5. *Saturations and bulk volumes estimation*

Archie, 1942 is used to calculate the water saturation (S_w) and consequently the hydrocarbon saturation (S_h), equations (4.5a & 4.5b). By knowing the porosity, the bulk volume of water (BVW) and the bulk volume of hydrocarbon (BVH) can be estimated by multiplying the porosity with the saturation values, equations (4.5c & 4.5d).

Water and hydrocarbon saturations are show in Fig (4.5), as well as the bulk volumes of water and hydrocarbon in WD38-1 well, as an example.

$$S_w = \sqrt{FR_w * \left(\frac{1}{R_t} - \frac{V_{sh}}{R_{sh}}\right)} \quad (4.5a)$$

$$S_{xo} = \sqrt{FR_{mf} * \left(\frac{1}{R_{xo}} - \frac{V_{sh}}{R_{sh}}\right)} \quad (4.5b)$$

where:

S_w&S_{xo} are the water saturations in the uninvaded zone and the invaded zone respectively; $R_w$is the formation water resistivity. R_t is the true formation resistivity; R_{mf} is the mud filtrate resistivity; R_{xo} is the invaded zone resistivity; F is the formation resistivity factor; $V_{sh}$is the corrected volume of shale; R_{sh} is the resistivity of shale.

Now, by calculating the water saturation, the hydrocarbon saturation can be estimated from equations (4.5c - 4.5e).

$$S_h = 1 - S_w \quad (4.5c)$$

$$S_{hr} = 1 - S_{xo} \quad (4.5d)$$

$$S_{hm} = S_h - S_{hr} \quad (4.5e)$$

where:

S_h is the hydrocarbon saturation in the uninvaded zone; $S_{hr}$is the residual hydrocarbon saturation in the invaded zone; $S_{hm}$is the movable hydrocarbon saturation (producible) in the connected pores.

By knowing the porosity ($\emptyset$), water saturation (S_w) and the hydrocarbon saturation (S_h), the bulk volume of water (BVW) and the bulk volume of hydrocarbon could be estimated, where (BVW) is the product of the porosity and the water saturation (equation 4.5f) similarly (BVH) is the product of the porosity and hydrocarbon saturation (equation 4.5g).

$$BVW = \emptyset * S_w \quad (4.5f)$$

$$BVH = \emptyset * S_h \quad (4.5g)$$

where:

BVW is the bulk volume of water; BVH is the bulk volume of hydrocarbon.

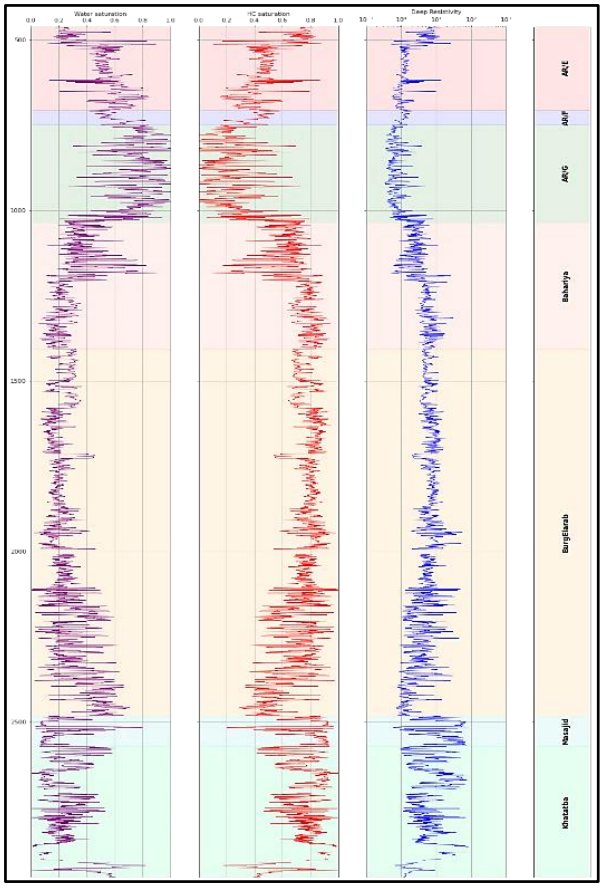

Fig.4.5. Curves for water saturation (Sw), effective porosity and bulk volume of water (BVW) in WD38-1 well.

4.6. *Litho-saturation model*

The litho-saturation models for all wells are constructed, which provide a direct method for representing the most important petrophysical parameters (V_{sh}, $\emptyset$, V_{ma}, BVW and BVH) at each depth in each well. Figure (4.6a) shows the litho-saturation model for WD38-1 well.

4. Results

The outcome of the petrophysical evaluation showed that, this area has a very promising hydrocarbon reservoir. WD38-1 well showed that, the lower Bahariya Formation contains a promising net-pay reservoir. WD38-1 well showed that, the hydrocarbon is present in Lower Bahariya Formation and in the Upper Burg El Arab Formation The highest net-pay zone is 180 m. at the Lower Bahariya Formation, while the lowest is 120 m. at the upper Burg El Arab Formation (Fig 4.6b).

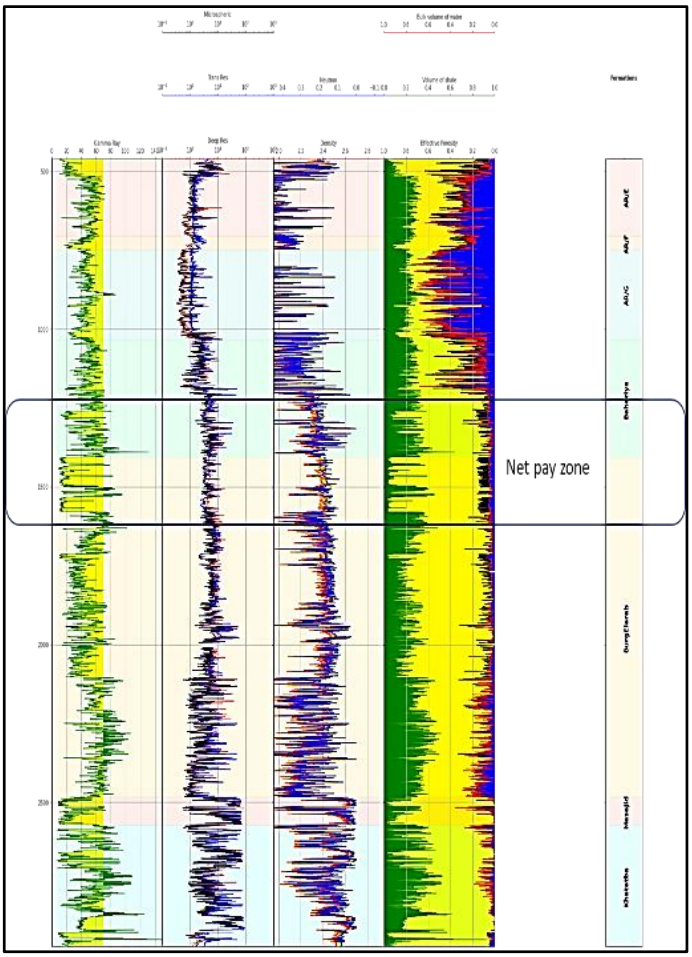

Fig.4.6a: Litho-saturation model for WD38-1 well.

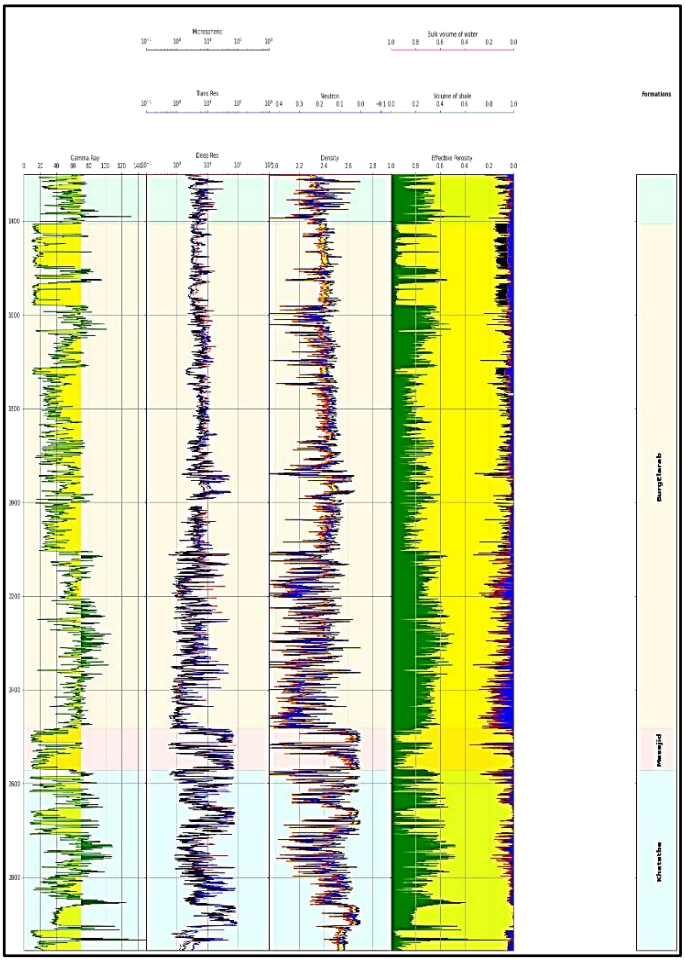

Fig. 4.6b: Litho-saturation model for the Bahariya reservoir in WD38-1 well.

WD38-1 well showed that, the average hydrocarbon saturation is 75% at the Lower Bahariya Formation, while the average hydrocarbon saturation is 87% at the Upper Burg El Arab Formation.

5. Conclusion

This paper displays a full petrophysical evaluation, aiming to improve the reservoir saturation of West Wadi El Rayan area. From the interpretation, the following conclusions have been reached:

1. The main reservoir in West Wadi El Rayan concession is the Lower Bahariya Formation and Upper Burg El Arab Formation. From the lithology cross plot, it consists mainly of sandstone mixed with few lime-stones.
2. The average total porosity is 20-25% and the average effective porosity is 15-18%, indicating a good reservoir quality.
3. From the hydrocarbon indicators and petrophysical parameters calculation, the hydrocarbon is present at WD38-1 well in the Lower Bahariya Formation, and in the Upper Burg El Arab Formation. This might be due to a structural feature event (maybe normal fault), causing the oil to be trapped in the Upper Burg El Arab Formation and in the Lower Bahariya Formation.

Declaration of Competing Interest

The authors declare that they have no conflict of interest.

Data availability

Data will be made available on request

6. References

Archie, G., 1942. The Electrical Resistivity Log as an Aid in Determining Some Reservoir Characteristics. Petroleum Transactions of the AIME, 146, pp. 54-62.

Asquith, G. and Daniel K., 2004. Basic well log analysis. AAPG. Print.

Asquith G. and Gibson, C., 1982. Basic well log analysis for geologists. AAPG, Tulsa, 216 pp.

Chikiban B., Kamel M. H., Mabrouk W. M. and Metwally A., 2022. Petrophysical characterization and formation evaluation of sandstone reservoir: Case study from Shahd field, Western Desert, Egypt. Contributions to Geophysics and Geodesy, Vol. 52/3, 2022 (PP.443-466).

Darwish (1992). Phanerozoic passive margins, cratonic basin and global tectonic maps and sedimentary basin of Egypt

Doveton, J., 1994. Geologic Log Analysis Using Computer Methods, AAPG Computer Applications in Geology 2.

Egyptian General Petroleum Corporation "EGPC" (1992): Western Desert, oil and Gas fields, A comprehensive overview. 11th EGPC Explor.and Prod. Conf. Cairo. PP. 1-431.

Hassan A. M., Mabrouk W. M., Farhoud K. M., 2013: Petrophysical analysis for Ammonite-1 well, Farafra Area, Western Desert, Egypt. Egy. J. Appl. Geophys., Vol. 19, No. 1

Hassan A. M., Abuzaeid M. S., Mabrouk W. M., Khalil M. H., 2019: Petrophysical analysis for the well logging data; Case study from Matruh basin, Western Desert, Egypt. Arab. J. Geosci., 7, 12, 5107{ 5125, doi:10.1007/s12517-013-1123-y.

Kamel MH, Mabrouk WM (2003), Estimation of shale volume using a combination of the three porosity logs. J Pet Sci Eng 40:145–157

Luthi, S., 2001. Geological Well Logs. Springer-Verlag Berlin.

Pickett, G., R., 1973. Pattern recognition as a means of formation evaluation: The Log Analyst, vol. 14, no. 4, PP. 3–11.

Said, R. (1962). The Geology of Egypt. Elsevier, Amsterdam-New York. 377 P.

Said, R. (1990). Cretaceous paleogeographic maps. In Said, R. (ed.). The Geology of Egypt. Balkema-Rotterdam-Brookfield. PP. 439-449.

Schlumberger, 1972. Log interpretation: volume 1—principles. Schlumberger Well Services, Houston, p.113.